Geochemistry Geophysics Geosystems G3

AN ELECTRONIC JOURNAL OF THE EARTH SCIENCES

Published by AGU and the Geochemical Society

Article

Volume 8, Number 11

13 November 2007

Q11002, doi:10.1029/2006GC001509

ISSN: 1525-2027

Young volcanism and related hydrothermal activity at 5°S on the slow-spreading southern Mid-Atlantic Ridge

K. M. Haase

Institut für Geowissenschaften, Abteilung Geologie, Christian-Albrechts-Universität zu Kiel, Olshausenstr. 40, D-24118 Kiel, Germany

Now at Department of Earth Sciences, University of Aarhus, Høegh-Guldbergs Gade 2, 8000 Aarhus C, Denmark

S. Petersen

Leibniz Institute of Marine Sciences (IFM-GEOMAR), Wischhofstr. 1-3, D-24148 Kiel, Germany

A. Koschinsky

School of Engineering and Science, International University Bremen IUB, Campus Ring 8, D-28759 Bremen, Germany

R. Seifert

Institut für Biogeochemie und Meereschemie, Universität Hamburg, Bundesstr. 55, D-20146 Hamburg, Germany

C. W. Devey, R. Keir, K. S. Lackschewitz, B. Melchert, M. Perner, O. Schmale, and J. Süling

Leibniz Institute of Marine Sciences (IFM-GEOMAR), Wischhofstr. 1-3, D-24148 Kiel, Germany

N. Dubilier and F. Zielinski

Max-Planck-Institut für Marine Mikrobiologie, Celsiusstr. 1, D-28359 Bremen, Germany

S. Fretzdorff, D. Garbe-Schönberg, and U. Westernströer

Institut für Geowissenschaften, Abteilung Geologie, Christian-Albrechts-Universität zu Kiel, Olshausenstr. 40, D-24118 Kiel, Germany

C. R. German, T. M. Shank, and D. Yoerger

Woods Hole Oceanographic Institution, Woods Hole, Massachusetts 02543-1050, USA

O. Giere

Max-Planck-Institut für Marine Mikrobiologie, Celsiusstr. 1, D-28359 Bremen, Germany

J. Kuever

Department of Microbiology, Bremen Institute for Materials Testing, Paul-Feller-Str. 1, D-28199 Bremen, Germany

H. Marbler and J. Mawick

School of Engineering and Science, International University Bremen IUB, Campus Ring 8, D-28759 Bremen, Germany

C. Mertens, U. Stöber, and M. Walter

Institut für Umweltphysik, Universität Bremen, Otto-Hahn-Allee, D-28359 Bremen, Germany

C. Ostertag-Henning
Bundesanstalt für Geowissenschaften und Rohstoffe, Stilleweg 2, D-30655 Hannover, Germany

H. Paulick
Mineralogisch-Petrologisches Institut, Universität Bonn, Poppelsdorfer Schloss, D-53115 Bonn, Germany

M. Peters and H. Strauss
Geologisch-Paläontologisches Institut, Universität Münster, Corrensstraße 24, D-48149 Munster, Germany

S. Sander
Department of Chemistry, University of Otago, P.O. Box 56, Dunedin, New Zealand

J. Stecher
Forschungsinstitut und Naturmuseum Senckenberg, Senckenberganlage 25, D-60325 Frankfurt, Germany

M. Warmuth and S. Weber
Institut für Biogeochemie und Meereschemie, Universität Hamburg, Bundesstr. 55, D-20146 Hamburg, Germany

[1] The effect of volcanic activity on submarine hydrothermal systems has been well documented along fast- and intermediate-spreading centers but not from slow-spreading ridges. Indeed, volcanic eruptions are expected to be rare on slow-spreading axes. Here we report the presence of hydrothermal venting associated with extremely fresh lava flows at an elevated, apparently magmatically robust segment center on the slow-spreading southern Mid-Atlantic Ridge near 5°S. Three high-temperature vent fields have been recognized so far over a strike length of less than 2 km with two fields venting phase-separated, vapor-type fluids. Exit temperatures at one of the fields reach up to 407°C, at conditions of the critical point of seawater, the highest temperatures ever recorded from the seafloor. Fluid and vent field characteristics show a large variability between the vent fields, a variation that is not expected within such a limited area. We conclude from mineralogical investigations of hydrothermal precipitates that vent-fluid compositions have evolved recently from relatively oxidizing to more reducing conditions, a shift that could also be related to renewed magmatic activity in the area. Current high exit temperatures, reducing conditions, low silica contents, and high hydrogen contents in the fluids of two vent sites are consistent with a shallow magmatic source, probably related to a young volcanic eruption event nearby, in which basaltic magma is actively crystallizing. This is the first reported evidence for direct magmatic-hydrothermal interaction on a slow-spreading mid-ocean ridge.

Components: 8945 words, 9 figures, 3 tables.

Keywords: mid-ocean ridge; eruption; vent fauna; fluids; phase separation.

Index Terms: 1032 Geochemistry: Mid-oceanic ridge processes (3614, 8416); 0450 Biogeosciences: Hydrothermal systems (1034, 3017, 3616, 4832, 8135, 8424); 1034 Geochemistry: Hydrothermal systems (0450, 3017, 3616, 4832, 8135, 8424).

Received 13 October 2006; **Revised** 20 June 2007; **Accepted** 29 August 2007; **Published** 13 November 2007.

Haase, K. M., et al. (2007), Young volcanism and related hydrothermal activity at 5°S on the slow-spreading southern Mid-Atlantic Ridge, *Geochem. Geophys. Geosyst.*, *8*, Q11002, doi:10.1029/2006GC001509.

1. Introduction

[2] At spreading rates above about 20 mm/a, mid-ocean ridge volcanism creates a dominantly magmatic crust 6–8 km thick [*White et al.*, 1992; *Dick et al.*, 2003]. As a result, the frequency of magmatic events might be expected to be generally lower on slow-spreading ridges as less crust is created here per unit time. In contrast to fast spreading ridges, however, volcanism (and mantle upwelling) on slow-spreading ridges seems to be focused at discrete volcanic centers, often near the center of segments [*Lin et al.*, 1990], suggesting that although the average rate of volcanism is lower on slow-spreading ridges, active volcanism might be concentrated at certain "hot spots" along the ridge.

[3] Cooling of magmatic rocks forming the oceanic crust leads to hydrothermal venting which has been found on all spreading axes on Earth [*Baker and German*, 2004]. Recent magmatic events on fast- to intermediate-spreading axes in the Pacific Ocean have significant effects on the associated hydrothermal systems [*Delaney et al.*, 1998]. A general pattern for the response of these systems to a magmatic event has been suggested [*Butterfield et al.*, 1997; *Delaney et al.*, 1998] but its relevance for hydrothermal systems on slow-spreading axes is unknown. Hydrothermal vents host chemosynthetic ecosystems which can be divided into several biogeographic provinces on the basis of their fauna [*Van Dover et al.*, 2002]. The Mid-Atlantic Ridge (MAR) in the South Atlantic, although playing a key role in the global distribution of vent fauna and the chemical budget of the oceans, is amongst the least explored spreading axes. It has, for example, been speculated that the hydrothermal vent faunas in the South Atlantic may bear some resemblance to faunas from the East Pacific Ocean because of the connection through the Drake Passage [*Van Dover et al.*, 2002]. However, until recently very little was known even about the abundance of hydrothermal activity along this axis [*German et al.*, 2002; *Baker and German*, 2004].

[4] Here, we present results of a study on the first three hydrothermal vent fields discovered on the southern Mid-Atlantic Ridge [*German et al.*, 2005; *Haase and M64/1 Scientific Party*, 2005; C. R. German et al., Hydrothermal activity on the southern Mid-Atlantic Ridge: Tectonically- and volcanically-hosted venting, 2–7°S, submitted to *Earth and Planetary Science Letters*, 2007]. We show that two of these hydrothermal systems have been affected by a very recent volcanic intrusion and eruption event. Our results generally support the proposed model for the relation between volcanic and hydrothermal activity.

2. Methods

2.1. Sampling and Measurements From the Ship

2.1.1. Sampling of Rocks and Hydrothermal Sediments

[5] Volcanic rocks were sampled using a wax rock corer and additionally, lava samples were also recovered in several TV-guided grabs used to sample hydrothermal precipitates. Some of the rock samples recovered with the TV-guided grab also contained biological samples, for example, thin bacterial films which were studied on board under the microscope.

2.1.2. Water Column Measurements and Sampling

[6] Conductivity-temperature-depth (CTD) casts were carried out using a Sea-Bird Electronics, Inc. SBE 911plus system, additionally equipped with a Wet Labs LSS backscatter sensor (a Miniature Autonomous Plume Recorder (MAPR) [*Baker and Milburn*, 1997]) and a redox potential/Eh probe. The CTD sensors were calibrated at Sea-Bird Electronics in September 2004. The underwater unit was attached to a SBE 32 carousel water sampler with 22 Niskin bottles.

2.2. Sampling and Measurements Using a Remotely Operated Vehicle (ROV)

[7] The hydrothermal fields were observed and sampled using the "Quest4000m" remotely operated vehicle (ROV; MARUM, Bremen) equipped with several still and filming cameras and two manipulating arms. These arms were used to sample hydrothermal precipitates, e.g., from vents, biological samples and to pick up lava samples. Several additional measuring and sampling devices were installed on the ROV.

2.2.1. Hydrothermal Fluid Sampling

[8] A fully remotely controlled flow-through system, the Kiel Pumping System (KIPS-3), mounted on the tool sled of the ROV was used for in situ hydrothermal fluid sampling [*Garbe-Schönberg et al.*, 2006]. The parts of the system which come into contact with the sample are made entirely of inert materials: perfluoralkoxy (PFA) and polytetrafluorethylene (PTFE, Teflon®), and a short tube of high-purity titanium (99.9% Ti). Fluid enters via this titanium tube (50 cm length, 8 mm I.D., bent to 45°), the "nozzle." Parallel to the titanium nozzle is a high-temperature sensor (see below) delivering real-time temperature data for the tip of the nozzle. Coiled PFA tubing (3/8" O.D., 3 m length) connects the nozzle to a remotely controlled multiport valve (PETP/PTFE) through which fluid can be directed into up to nine different PFA sampling flasks with 675 mL volume each (Savillex, USA). These flasks are flow through and the flasks' exits are closed by check valves. Flasks were pre-filled with ambient bottom seawater obtained from CTD hydrocasts prior to deployment. The pumping rate can be adjusted to fluid flow rate; the standard

pumping time per sample was set to 4–5 min making sure that the flask volume was exchanged at least four times. The outlet of the KIPS system is located on the porch at the front-side of the ROV, where video control allows the observation of warm fluids leaving the system.

2.2.2. Fluid Temperature Measurements (Attached to KIPS; See Above)

[9] A high-precision thermistor temperature sensor (manufactured by H.-H. Gennerich, Bremen) inside a stainless steel pressure housing was attached parallel to the KIPS nozzle. The sensor was connected to the ROV's modified CTD-60_77 (Sea and Sun, Trappenkamp, Germany) using two channels for data handling: a broadband channel for temperatures <100°C, and a dedicated high-temperature channel for the range 100–450°C. The 90% time constant of the sensor in water is better than 12 s. A pre-cruise calibration was performed with the CTD-60_77 housing equilibrated to 2.4°C water temperature, simulating in-situ conditions during the cruise.

2.3. Analytical Methods

2.3.1. Methane Analysis

[10] Samples for the determination of dissolved hydrogen and methane were obtained on board by connecting 50 to 250 ml of sample to a high grade vacuum as described by *Rehder et al.* [1999]. Briefly, the water samples were drawn from the KIPS sample bottle into an evacuated 500 mL bottle and the gas effervesced into the gas phase was then transferred to a gas burette. Aliquots of the released gas taken via a septum from the burette and injected into the analytical units by gas tight syringes. A gas chromatograph (CARLO ERBA GC 6000) equipped with a packed (activated Al_2O_3) stainless steel column and a flame ionization detector (FID) is used to detect and quantify methane after injection on column. The gas chromatograph temperature was 140°C and precleaned He was used as carrier gas. Hydrogen was analyzed by a gas chromatograph (Finnigan Thermoquest Trace GC) equipped with a molecular sieve 5A column (3 m × 1/8" 60/80 mesh) and a pulsed-discharge-helium-ionization detector (VICI PDD). The injection was done via a sample valve (0.5 or 1.5 mL sample) at an isothermal gas chromatograph temperature (40°C) with precleaned He as carrier gas. Recording and calculation of results was performed using a PC operated integration system (BRUKER Chrom Star). All analytical procedures were calibrated daily with commercial gas standards (LINDE).

2.3.2. Fluid Chemical Analysis

[11] Cl, Mg and Si in the fluid samples were analyzed by ICP-OES and are presented in Table 2. The M64/1 samples were not filtered and not acidified on board, but diluted and acidified (tenfold diluted with 2% HNO_3) prior to ICP-OES analysis using a Spectro "CIROS SOP" instrument on land. Results for Cl were double-checked by titration with $AgNO_3$. The M68/1 samples were not filtered but acidified on board with HNO_3 to pH 2, and diluted tenfold with 2% HNO_3 prior to land-based ICP-OES analysis.

2.3.3. Analysis of Hydrothermal Precipitates

[12] Selected samples were powdered using agate ball-mills and analyzed by XRD for their mineralogy. Polished thin sections were used for additional mineral identification using reflected and transmitted light microscopy.

3. Geological Setting

[13] South of the large, left-stepping Equatorial fracture zones, the Mid-Atlantic Ridge is divided into numerous segments of 100–200 km length separated by smaller (~50 km) or larger (200–300 km, e.g., Ascension Fracture Zone) offset transform faults. The segment discussed in this paper is approximately 120 km long and characterized by a pronounced axial high near the segment middle (Figure 1). The southern flank of this high was imaged in detail during a geophysical study [*Reston et al.*, 2002]. Water depths at the segment ends exceed 4500 m, the median valley floor at its shallowest around 4°48′S forms a ~10 km wide, hourglass shaped plateau with water depths of around 3000 m (Figure 1). Full spreading rates are about 32 mm/a [*De Mets et al.*, 1990] and the sedimentation rate in the area is about 32 mm/ka [*Ruddiman and Janecek*, 1989]. Most of the lavas on the plateau are aphyric sheet flows and pillows. Collapse structures with lava pillars are frequent in the sheet flows (Figures 2a and 2b). The predominance of only slightly altered to very fresh lavas and unsedimented sheet flows (Figures 2c, 2d, and 2e) on this high implies recent and strong volcanic activity and high eruption rates in this segment of the Mid-Atlantic Ridge. Pillow lavas occur only in a few areas (Figure 2f), but can also form

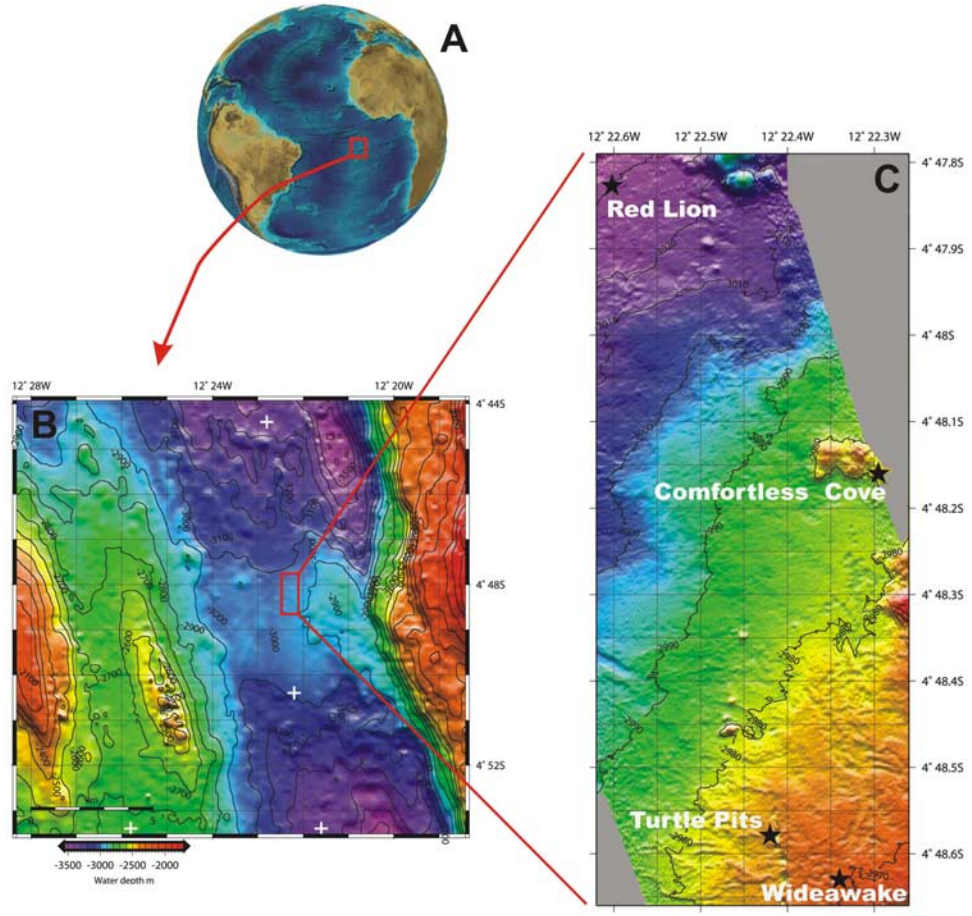

Figure 1. (a) Location of the working area and (b) bathymetric map of the rift valley of the southern Mid-Atlantic Ridge at 4°48′S. The white crosses denote the location of earthquakes of the 25–26 June 2002 seismic crisis in the area. (c) The ABE bathymetric map showing the location of the three high-temperature hydrothermal vent sites as well as the Wideawake diffuse vent field (black stars).

substantial pillow mounds. One low-temperature vent field (Wideawake) and three closely spaced high-temperature vent fields (Turtle Pits, Red Lion and Comfortless Cove, see description below) were found on a flat (total relief 50 m), volcanically and tectonically active 2 km section of this plateau (Figure 1) [*German et al.*, 2005; *Haase and M64/1 Scientific Party*, 2005]. The Turtle Pits site lies within laminated and jumbled sheet flows, reminiscent of fast spreading ridges, whereas the seafloor around Comfortless Cove and Red Lion is characterized by pillow lavas. A very fresh lava flow occurs on the eastern rim of the Wideawake diffuse field and in some areas this pillow lava flow covers the hydrothermal fauna (Figures 2e and 3), i.e., is clearly younger than the organisms.

4. Description of Hydrothermal Sites

[14] The northernmost site is the Red Lion hydrothermal field which is centered at 4°47.83′S/12°22.60′W in a water depth of 3050 m and consists of at least four active black smoker chimneys separated by only 10–15 m and emplaced directly on a pillow lava flow (Figure 4a). Three of the smokers (“Mephisto,” “Sugarhead,” and “Tannenbaum”; Table 1) are typical 4–6 m high pillar-like structures, whereas the fourth, called “Shrimp Farm,” is a 4 m high structure with a 5 m wide plateau of extreme flange growth at the top (Figure 5a). The sulfides consist of chalcopyrite-pyrite-sphalerite. Red Fe-oxyhydroxides cover the area adjacent to the active vents. Several inactive vents were also observed in the surrounding area of the active vent field but the lack of abundant hydrothermal sediment suggests that this field is relatively young, although recrystallized massive sulfides are obvious at the base of the sulfide structures. The fauna is dominated by large swarms of the vent shrimp *Rimicaris exoculata*, while other shrimps (*Mirocaris* sp.) and crabs (probably *Segonzacia* c.f. *mesatlantica*) are rare.

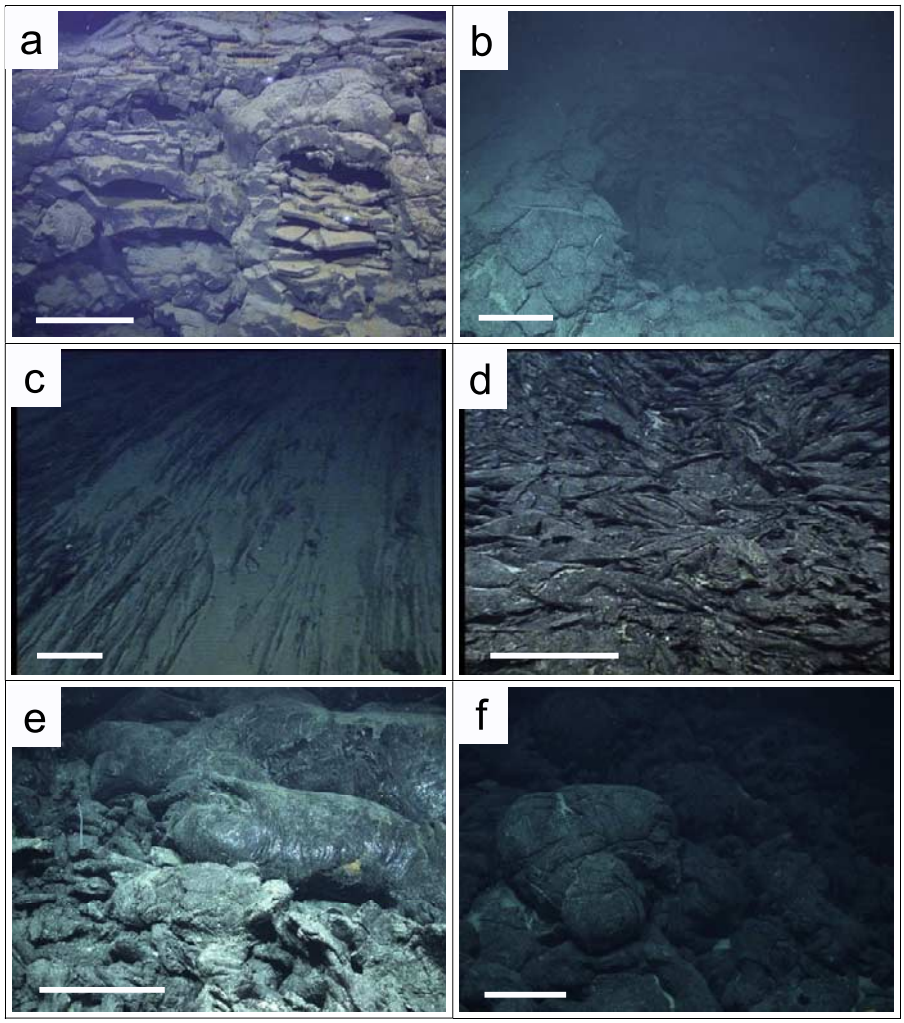

Figure 2. Bottom still photographs of lava morphologies in the vicinity of the hydrothermal fields at 5°S (photos courtesy of MARUM, University of Bremen). (a) Cliff with lava tubes showing plates of sinking lava level. The cliff is exposed at the eastern inner wall of the Turtle Pits main pit. (b) Collapse pits along the northern extension of the fault hosting the Turtle Pits hydrothermal field. (c) Slightly sedimented sheet flows to the west of Turtle Pits. (d) Hackly sheet flows to the east of Turtle Pits. (e) Fresh, glassy lava tongues covering older hackly sheet flows at the Wideawake diffuse field. (f) Pillow lava on the mound adjacent to the Comfortless Cove hydrothermal field. Scale bars are ~0.5 m.

Interestingly, the wide platform of the Shrimp Farm vent was densely populated by shrimp in 2005, whereas hardly any shrimps were observed on this structure in 2006. The end-member chlorinity of the Red Lion vent fluids is 546 mmol/L (Table 2), which is close to seawater salinity. This chlorinity is consistent with the visual observations on the smoker themselves, as no evidence was seen for boiling. End-member gas concentrations calculated from fluid samples obtained in 2005 are 0.12 and 0.041 mmol/L for H_2 and CH_4, respectively. The Si concentration of the end-member fluids is 21 mmol/L, comparable to typical fluids from basalt-hosted hydrothermal vents [*Von Damm*, 1995].

[15] Comfortless Cove is situated at 4°48.19′S/12°22.30′W in a water depth of 2996 m approximately 70 m southeast of a prominent pillow mound (Figures 1b and 4b). The active vent (named "Sisters Peak") is 13 m high and consists of two spires (Figure 5b). The base of the chimney is characterized by blocks of recrystallized massive sulfides that are colonized by mussels, crabs and shrimps which were sampled for taxonomic studies. A sulfide pile at the eastern base of the chimney is covered by a very fresh and probably young lava flow. The eastern spire of this smoker is inactive, whereas the west spire is venting acidic (pH 3.1) low-salinity fluids with a calculated end-member composition of 224 mmol/L Cl and 14.5 mmol/L Si.

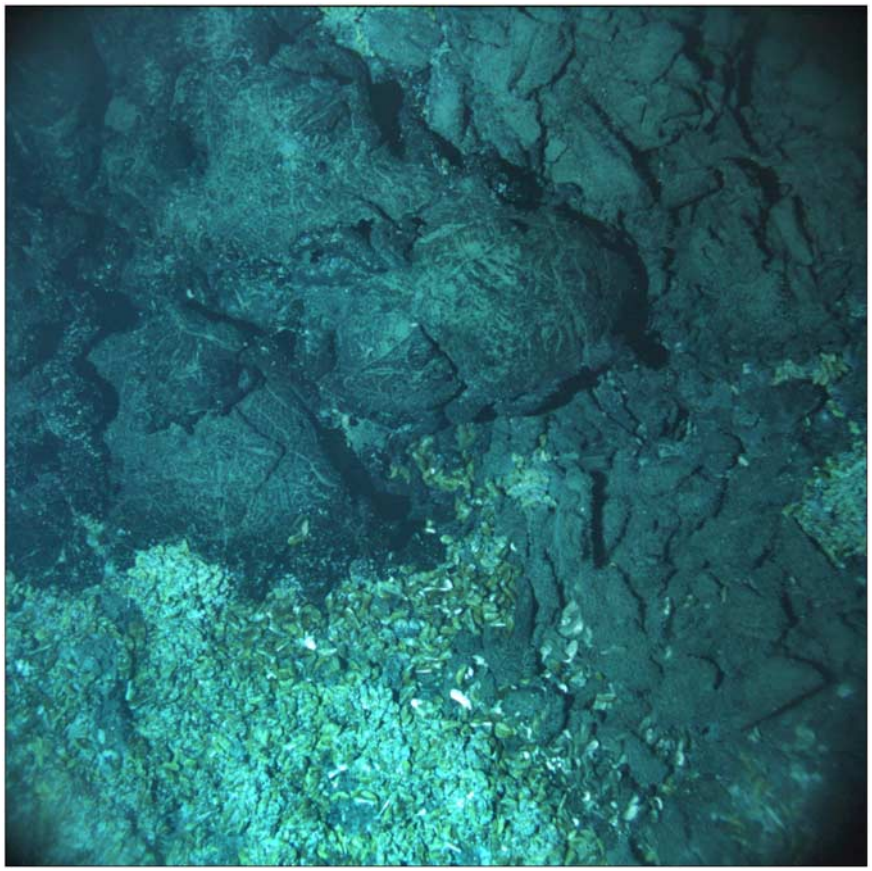

Figure 3. Downward looking photograph taken by the ABE autonomous underwater vehicle of fresh lava flows (top left) engulfing hydrothermal *Bathymodiolus puteoserpentis* mussel beds (yellow bivalves) and anemones (white) that mottle the surfaces of older lava flows in the Wideawake diffuse field.

The measured maximum exit temperature was 400°C (Table 1). Two diffuse venting sites occur in close neighborhood to Sisters Peak. The Golden Valley diffuse vent site with a measured temperature of 3.6°C is located in a N-S oriented fissure 70 m northeast of Sisters Peak and stretches for 30 m. The walls and the bottom of the fissure are intensely colonized by mussels whose golden-brown chitinous covering gave rise to the name (Figure 5c). Another diffuse vent field lies approximately 60 m to the northwest of Golden Valley, almost due north from Sisters Peak. The size of the field is 10 m × 20 m and it is characterized by abundant patches of mussel beds and a diffuse venting of fluids with temperatures up to 10°C. The cloudy water that characterizes this area led us to name it "Foggy Corner." End-member gas concentrations calculated from fluid samples taken from Sisters Peak in 2006 are 0.061 mmol/L H_2 and 0.013 mmol/L CH_4.

[16] The Turtle Pits field is situated 1 km further south (4°48.58′S/12°22.42′W) in a water depth of 2990 m on the flank of a volcanic edifice in the center of the segment. The Turtle Pits site lies within a small depression associated with a fracture marked by aligned collapse pits (Figure 4c), a setting similar to those of many hydrothermal vents on the fast spreading East Pacific Rise [*Fornari et al.*, 2004]. The central depression is surrounded by laminated sheet flows to the north and northwest, whereas jumbled flows are more prevalent to the east. Turtle Pits is composed of a large active black smoker chimney (called Southern Tower, Figure 6) whose height increased from about 9 m in April 2005 to about 13 m in May 2006 (determined by using the bottom-seeking sonar of the ROV and hovering at the top of the chimney) and two mounds of sulfide debris that are capped by numerous small active black smokers (sites "One Boat" and "Two Boats"). Vigorously venting fluids at these two mounds are characterized by gas bubbles (Figure 5d and Movie 1)[1] indicating, at this water depth, phase separation close to the

[1]Movie 1 is available in the HTML.

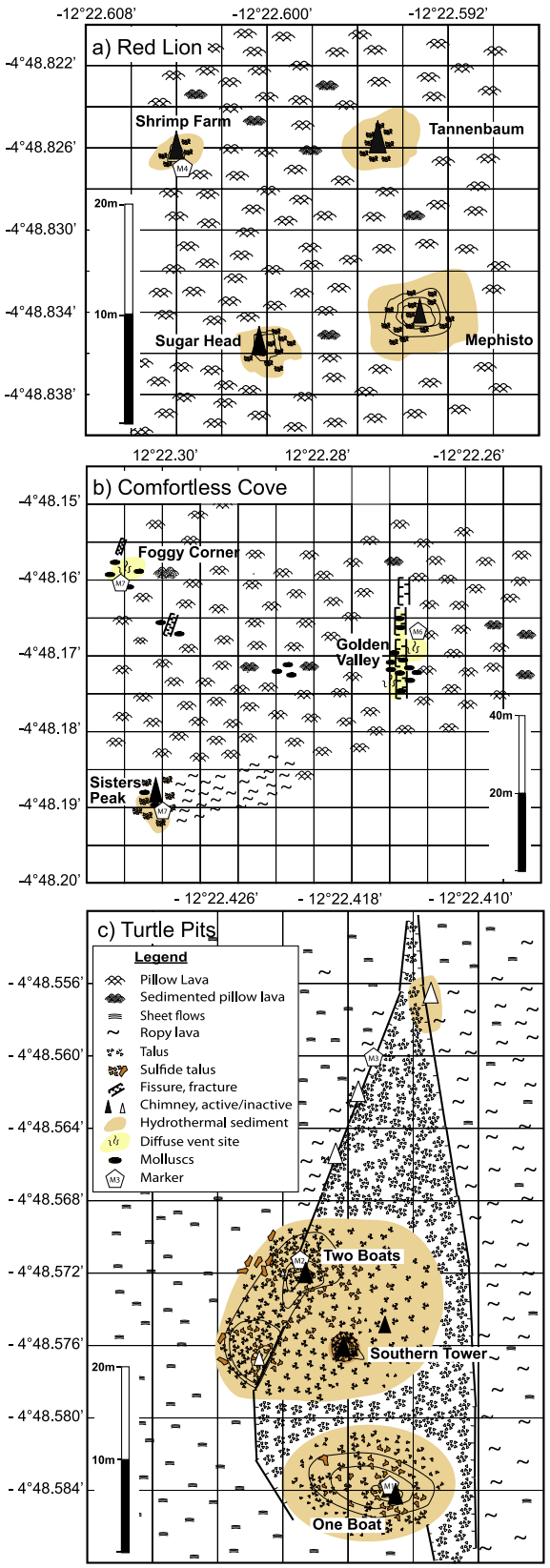

Figure 4. Sketch maps of the three newly described hydrothermal vent fields showing the geological setting and location of active and inactive hydrothermal sulfide chimneys: (a) Red Lion field, (b) Comfortless Cove field, and (c) Turtle Pits field. Note the different length scale for each field.

critical point of seawater (407°C, 298 bar [*Bischoff and Rosenbauer*, 1988]). This is in agreement with measured fluid exit temperatures of 407°C, the highest temperature measured anywhere along the mid-ocean ridges. Both standing and collapsed inactive sulfide chimneys were observed at the edge of the volcanic collapse pit containing the presently active vents. The inactive chimneys and mass wasting of sulfides suggest previous periods of hydrothermal activity.

[17] The active black smokers at Turtle Pits are characterized by a pyrrhotite-chalcopyrite-isocubanite mineral assemblage suggesting conditions close to the pyrite-pyrrhotite-magnetite (PPM) redox buffer [*Von Damm et al.*, 1995] in the reaction zone (Figure 7). In contrast, the presence of primary hydrothermal hematite-magnetite-pyrite in inactive massive sulfides and chimney talus from immediately northwest of the current vents indicates that more oxidized conditions prevailed in the past. The presence of abundant hematite in association with magnetite and pyrite (Table 3) as seen at Turtle Pits has not been described before from a seafloor hydrothermal system, and such oxidizing conditions were previously unknown in basalt-hosted mid-ocean ridge vent sites [*Seyfried et al.*, 2004]. Massive blocks of white material containing anhydrite and some talc are exposed along the northwestern side of the "Two Boats" site and in the pit itself.

[18] The sulfide chimneys at Turtle Pits are less densely populated with shrimps and crabs when compared to those at Red Lion. Small patches of vent mussel shells of (*Bathymodiolus puteoserpentis*) were observed outside the collapse pits at Turtle Pits close to the inactive smokers.

[19] A minimum pH value of 3.1 was measured in the Turtle Pits vent fluids (Table 1) which is identical to that measured in the Sisters Peak vent fluids. The end-member chlorinity remained constant at about 270 mmol/L Cl between 2005 and 2006, slightly higher than the Comfortless Cove vent fluid but still significantly reduced relative to ambient seawater (~560 mmol/L Cl) (Table 1 and Figure 8a). This indicates that the fluids are phase-separated and that the samples represent the vapor

Table 1. Location, Water Depths, Fluid Temperatures, pH, and Gas Concentrations of Active Black Smokers in the Hydrothermal Vent Fields at 4°48′S[a]

Vent Field/ Structure	Latitude	Longitude	Water Depth, m	Temperature, °C	pH	H_2, mmol/L	CH_4, mmol/L
			Turtle Pits Field				
Two Boats	4°48.573′S	12°22.421′W	2985	407 (May 2006) 400 (April 2005)	3.1	0.664	0.045
Southern Tower	4°48.579′S	12°22.419′W	2990	n.d.	n.d.	n.d.	n.d.
One Boat	4°48.588′S	12°22.414′W	2986	n.d.	n.d.	n.d.	n.d.
			Comfortless Cove Field				
Sisters Peak	4°48.188′S	12°22.301′W	2996	400	3.1	0.061	0.013
			Red Lion Field				
Tannenbaum	4°47.826′S	12°22.595′W	3046	348	n.d.	n.d.	n.d.
Shrimp Farm	4°47.827′S	12°22.604′W	3047	193	n.d.	n.d.	n.d.
Mephisto	4°47.834′S	12°22.593′W	3045	346	5.5	0.12	0.041
Sugarhead	4°47.836′S	12°22.600′W	3046	n.d.	n.d.	n.d.	n.d.

[a] Notes: n.d., not determined. Turtle Pits and Red Lion gas data are from April 2005 (M64/1 141 and 146 ROV), and Comfortless Cove gas data are from May 2006 (M68/1 20 ROV).

phase of a boiling system. The Turtle Pits hydrothermal end-member fluid also had low dissolved silica concentrations of about 11 mmol/L Si in 2005 and 2006 (Figure 8b) when compared to most known hydrothermal end-member fluids. However, similar low Si concentrations have been observed in the vapor phase of boiling vents on the East Pacific Rise that are affected by recent volcanic activity [*Von Damm et al.*, 1995]. Hydrogen and methane concentrations in the fluid end-member are 0.66 mmol/L H_2 and 0.045 mmol/L CH_4. While H_2 concentrations are on the higher end of values from basalt-hosted systems (Figure 9), the CH_4 values are rather low.

[20] Some 200 m to the east of Turtle Pits, diffuse venting in the Wideawake field occurs in a jumbled sheet flow. The southeastern part of the diffuse-venting field is covered by unsedimented pillow lavas with a highly vitreous luster (Figures 2e and 3) suggesting a very recent volcanic eruption (compare, e.g., *Chadwick and Embley* [1994]). The fauna is more diverse than at the high temperature site, consisting mainly of vent mussels (*Bathymodiolus puteoserpentis*), patches of vesicomyid clams (*Calyptogena* sp., Figures 5e and 5f), occasional *Rimicaris exoculata,* conid snails (?*Phymorhynchus* sp.), and limpets (Neolepetopsidae). Colorless H_2S-oxidizing bacteria (identified on the basis of the presence of sulfur globuli as well as typical morphology) were observed under the microscope on a lava sample recovered with the TV-guided grab close to *Bathymodiolus* assemblages. Some of the bacteria consist of white filaments and are up to 20 μm wide, typical morphological features of *Thiothrix* spp. [*Larkin and Shinabarger*, 1983]. Similar attached filamentous sulfur bacteria have been found at other submarine hydrothermal vents [e.g., *Jannasch*, 1983] and appear to be closely related to vacuolated *Beggiatoa* and *Thioploca* spp. [*Kalanetra et al.*, 2004]. White netlike structures were dominated by a large coccoid microorganism (20 μm width) similar to *Achromatium* spp. This is, to our knowledge, the first observation of *Achromatium sp.* at deep sea hydrothermal vents.

5. Discussion

5.1. Composition and Formation of the Vent Fluids

[21] Two of the three high-temperature sites (Turtle Pits and Comfortless Cove) are characterized by extremely high temperatures (407 and 400°C, respectively) and low chlorinities (~270 mmol/L at Turtle Pits and 222 mmol/L at Comfortless Cove; Table 2) indicating phase separation which, at a water depth of 2990 m, occurs at the critical point of seawater. The relationship between chlorinity and Mg contents of fluids from Turtle Pits and Comfortless Cove suggests that they have similar low-salinity, vapor-dominated end-member fluids; Wideawake also appears to lie on this trend (Figure 8a). Unlike the black smoker vents, the Wideawake fluids undergo extensive mixing with seawater during their ascent, reflecting either a higher permeability of the chaotic lava flows at this site, a separation of diffuse and focused upflow [*Lowell et al.*, 2003], or a difference in the evolutionary stage of the site. The latter process was

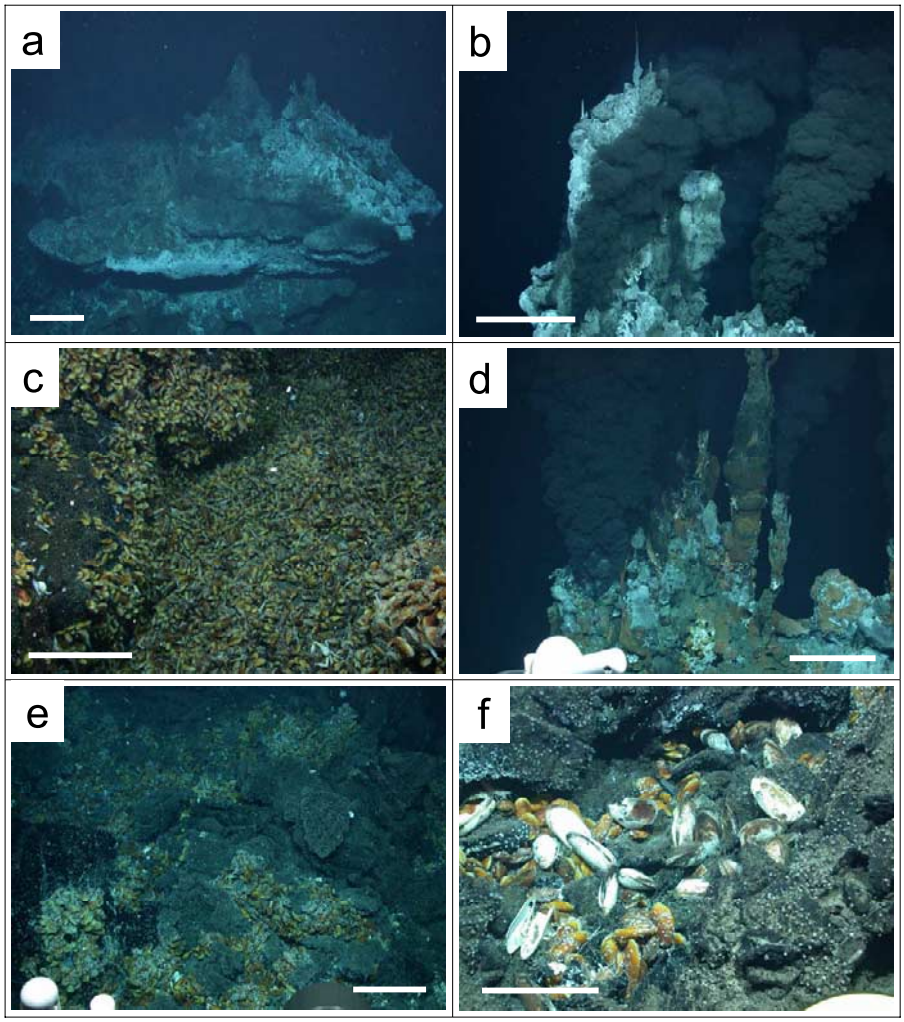

Figure 5. Bottom still photographs of vents fields at 4°48′S, MAR (photos courtesy of MARUM, University of Bremen). (a) Top of the smoker "Shrimp Farm" in the Red Lion hydrothermal field showing flange growth. (b) Upper part of the high-temperature (400°C) active chimney "Sisters Peak" at the Comfortless Cove vent field. (c) View of the "Golden Valley" diffuse field characterized by a dense population of *Bathymodiolus puteoserpentis*. (d) Smoker "Two Boats" at the Turtle Pits hydrothermal field. This vent shows bubbling which can be observed in Movie 1. (e) Mussel beds at the Wideawake diffuse field which are covered by a young lava flow on its eastern rim. (f) Assemblage of Vesicomyid clams (*Calyptogena* sp.) and Bathymodiolus puteoserpentis mussels in the Wideawake diffuse vent site. Scale bar is ~0.5 m.

reported immediately post-eruption at the 9°52′N area on the East Pacific Rise where extensive diffuse flow subsequently self-organized into discrete high-temperature vent systems in the years immediately following volcanic eruption [*Von Damm*, 2000].

[22] Compared to most global submarine hydrothermal vent fluids, the Turtle Pits fluids have elevated H_2 and low CH_4 concentrations (Figure 9 and Table 2), observations typical for post-eruptive hydrothermal systems on the Juan de Fuca Ridge and the East Pacific Rise [*Lilley et al.*, 2003]. The high H_2 contents in the fluids could be due to the gases being fractionated into the vapor phase during boiling, leading to relatively high concentrations, for example, of H_2 and CO_2 [*Butterfield et al.*, 1997], although the apparent preferential enrichment in H_2 relative to CH_4 in the Turtle Pits fluids is difficult to explain by this mechanism. Several mechanisms can, however, potentially lead to H_2 enrichment: We can rule out the hydrogen being formed by serpentinization of magmatic olivines [*Moody*, 1976] as the basalts at Turtle Pits are olivine-poor. Microbial activity [*Baross et al.*,

Table 2. Measured Compositions of Fluid Samples From Vents at 4°48′S and Calculated Fluid End-Member Compositions Assuming Mg = 0 mmol/L in the Fluid[a]

Cruise	Sample	Date	Method/Laboratory	Mg, mmol/L	Cl, mmol/L	Si, mmol/L
	seawater			54	560	0.04
			Red Lion			
M64/1	146ROV bottle1	16.4.2005	ICP-OES Kiel	52.5	560	0.05
M64/1	146ROV bottle2	16.4.2005	ICP-OES Kiel	54.2	559	0.06
M64/1	146ROV bottle3	16.4.2005	ICP-OES Kiel	54.5	564	0.05
M64/1	146ROV bottle4	16.4.2005	ICP-OES Kiel	56.2		0.05
M64/1	146ROV bottle5	16.4.2005	ICP-OES Kiel	53.8	563	0.07
M64/1	146ROV bottle6	16.4.2005	ICP-OES Kiel	52.8	560	n.d.
M64/1	146ROV bottle7	16.4.2005	ICP-OES Kiel	19.1	553	12.1
M64/1	146ROV bottle8	16.4.2005	ICP-OES Kiel	11.1	547	17.8
M64/1	146ROV bottle9	16.4.2005	ICP-OES Kiel	5.32	550	20.6
M64/1	146ROV bottle11	16.4.2005	ICP-OES Kiel	43.1	553	4.05
M64/1	146ROV bottle12	16.4.2005	ICP-OES Kiel	44.9	553	3.58
	calculated end-member				*545 (R^2 = 0.61)*	
M68/1	7ROV-4	11.5.2006	ICP-OES Kiel	38.4	551	4.56
M68/1	7ROV-5	11.5.2006	ICP-OES Kiel	49.6	556	1.2
M68/1	7ROV-11	11.5.2006	ICP-OES Kiel	51.7	558	0.2
M68/1	7ROV-13	11.5.2006	ICP-OES Kiel	45.4	558	2.2
						21.4
			Turtle Pits			
M64/1	123ROV bottle11	11.4.2005	ICP-OES Kiel	46.1	n.d.	1.22
M64/1	141ROV bottle12	15.4.2005	ICP-OES Kiel	27.7	419	4.82
M64/1	141ROV bottle13	15.4.2005	ICP-OES Kiel	27.0	417	4.72
M64/1	141ROV 12	15.4.2005	ICP-OES Kiel	34.3	459	3.28
M64/1	141ROV 13	15.4.2005	ICP-OES Kiel	31.3	446	4.86
M64/1	141ROV 14	15.4.2005	ICP-OES Kiel	30.7	445	4.34
M64/1	141ROV 15	15.4.2005	ICP-OES Kiel	24.1	396	6.74
	calculated end-member				*271 (R^2 = 1.00)*	*10.8 (R^2 = 0.95)*
M68/1	3ROV 10 K1	10.5.2006	ICP-OES Kiel	6.9	296	8.92
M68/1	12ROV 5 K2	12.5.2006	ICP-OES Kiel	2.8	290	11.03
M68/1	12ROV 8 K5	12.5.2006	ICP-OES Kiel	13.2	339	8.68
	calculated end-member				*267 (R^2 = 1.00)*	*11.1 (R^2 = 0.99)*
			Wideawake			
M64/1	125ROV bottle 11 1	12.4.2005	ICP-OES Kiel	46.5	505	n.d.
M64/1	125ROV bottle 11 2	12.4.2005	ICP-OES Kiel	46.9	505	n.d.
M64/1	125ROV bottle 12 1	12.4.2005	ICP-OES Kiel	49.2	524	n.d.
M64/1	125ROV bottle 12 2	12.4.2005	ICP-OES Kiel	49.5	519	n.d.
M68/1	3ROV 1 and 2	10.5.2006	ICP-OES Kiel	51.5	508	n.d.
			Comfortless Cove			
M68/1	20ROV 5 K6	14.5.2006	ICP-OES Kiel	38.1	459	4.30
M68/1	20ROV 6 K7	14.5.2006	ICP-OES Kiel	7.4	269	12.56
	calculated end-member				*222 (R^2 = 1.00)*	*14.5*

[a] Notes: n.d., not determined.

1982] probably does not occur at temperatures close to 400°C and can also be ruled out as a principal source for hydrogen in the vent fluids. Magmatic degassing of hydrogen [*Welhan and Craig*, 1979] is a possibility, as in a comparable setting to the southern MAR, i.e., at a spreading axis without sediment cover, H_2 and CO_2 concentrations in hydrothermal fluids increased significantly following the diking event at 9°N on the EPR [*Lilley et al.*, 2003]. However, CH_4 also showed a small but significant increase in the EPR vent fluids and thus we suggest that the most likely source for the high H_2 contents is the oxidation of Fe^{2+} to Fe^{3+} during cooling of basaltic magmas and reaction of the hot lava with seawater [*Christie et al.*, 1986; *Sansone et al.*, 1991].

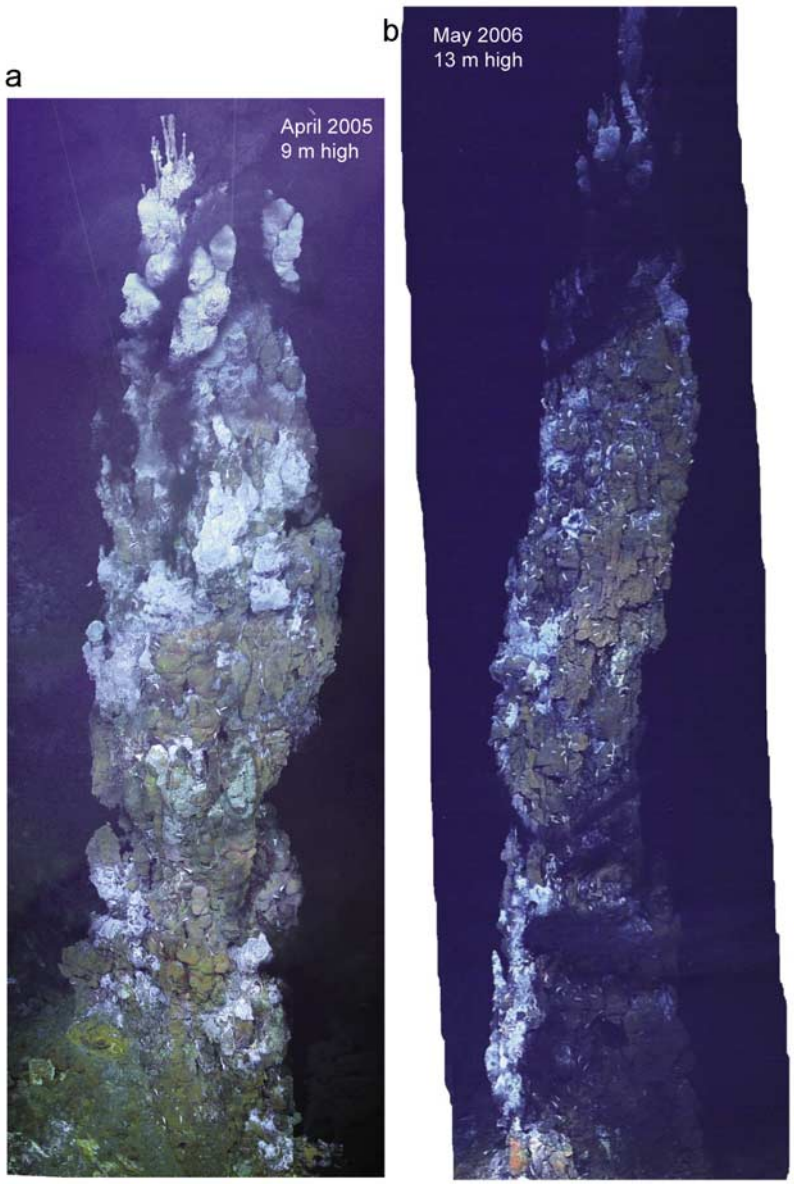

Figure 6. Photo mosaics of the "Southern Tower" vent in the Turtle Pits hydrothermal field (a) in April 2005 looking northward (0° heading) and (b) in May 2006 looking toward the NW (320° heading). The height of the structure increased from some 9 m in 2005 to about 13 m in 2006 as measured with the bottom sonar of the ROV by hovering at the top of the chimney. Note the strong bottom currents affecting the smokers near the base of the structure.

[23] Although the Turtle Pits and Comfortless Cove fluids appear, from their similar low salinities, to come from a similar, phase-separated source, they show significant differences in their H_2 contents. These are probably related to different extents of reaction with either seawater or the altered, oxidized upper crust during ascent, as H_2 is known to be extremely reactive in the deep ocean [*Ding et al.*, 2001]. The fact that the differences in H_2 between Comfortless Cove and Turtle Pits are not associated with differences in Mg-content of the fluids suggests that the reaction is not with seawater, and so we favor an interaction with the weathered upper crust to explain the H_2 differences. This in turn suggests that the crust immediately below Comfortless Cove is more weathered (older?) than that below Turtle Pits, in accordance with the occurrence of very recent, glassy lava near the Wideawake Field, just 300 m

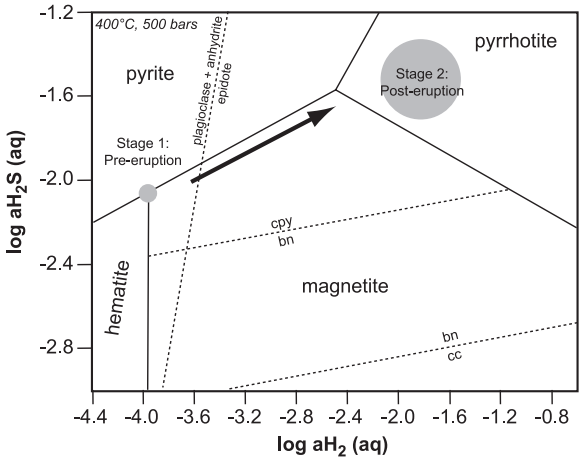

Figure 7. Modified phase diagram of magnetite-pyrite-pyrrhotite stability in basaltic seafloor hydrothermal systems [*Seyfried and Shanks*, 2004] showing the evolution of the hydrothermal fluids at Turtle Pits on the basis of the mineralogical composition of the inactive and active vents. The mineralogy of the presently active vents (Stage 2) suggests formation under redox conditions close to the pyrrhotite-pyrite-magnetite (PPM) buffer, whereas more oxidizing conditions beyond the anorthite-anhydrite-clinozoisite-pyrite-magnetite (AACPM) buffer prevailed during the earlier Stage 1 as is indicated by the mineral content of inactive chimneys (Table 3). This evolution is most likely due to the ascent of magma into the shallow crust as indicated by the very young lavas covering part of the Wideawake and Comfortless Cove hydrothermal fields. CPY, chalcopyrite; BN, bornite; CC, chalcocite.

southeast of the Turtle Pits vent site (see discussion below).

[24] The Si solubility in fluids can be used as a barometer provided their temperature and salinity are known [*Von Damm et al.*, 1995; *Foustoukos and Seyfried*, 2007]. The progressively increasing Si contents in the fluids from Turtle Pits, Comfortless Cove, and Red Lion suggest that the pressure of equilibration increases from south to north. Using the barometers given by *Foustoukos and Seyfried* [2007] and *Von Damm* [2000] we estimate that the depth of equilibration ranges from 340 bars at Turtle Pits to about 390 bars at Comfortless Cove and to more than 500 bars at Red Lion. Consequently, the reaction zone and most likely the magma body is very close to the seafloor (~150 m) beneath Turtle Pits but lies at a depth of perhaps 1 km at Red Lion. This very shallow intrusion below Turtle Pits and Comfortless Cove provides both the heat causing the phase separation of the fluids and, in the process, through cooling and iron oxidation, also releases H_2 into the fluids.

5.2. Evidence for Recent Volcanism on the MAR at 4°48′S

[25] Observations using the ROV and AUV show that the black fresh pillow lava with highly glassy luster (Figure 2e) covers the jumbled sheet flow with its diffuse venting and fauna at the eastern side of Wideawake (Figure 3). Furthermore, this lava is seen onlapping piles of sulfide debris at Comfortless Cove. Both observations provide field evidence for recent volcanic activity in the region. The high temperatures and vapor-dominated fluid compositions of the Turtle Pits and Comfortless Cove vent fields suggests that they have been influenced by this recent volcanic activity, whereas the Red Lion vent field, with its normal seawater salinity fluids and the much lower vent fluid exit temperatures, appears not to have been so strongly affected. Further evidence for recent volcanic influence at Turtle Pits comes from the sulfide mineralogy. As we have seen, the active black smokers at Turtle Pits are characterized by a mineral assemblage suggesting conditions close to the strongly reduced pyrite-pyrrhotite-magnetite (PPM) redox buffer [*Von Damm et al.*, 1995] while the presence of a mineral assemblage consisting of hematite-magnetite-pyrite in inactive chimney talus indicates that more oxidized conditions have occurred in the past (Figure 7). It has been shown both that fluid compositions can change to more reduced conditions immediately following an eruption [*Butterfield et al.*, 1997] and that these reduced fluids become progressively more oxidized as time passes after the eruption, e.g., at 9°46′N on the fast spreading East Pacific Rise and along the intermediate-spreading Juan de Fuca Ridge [*Haymon*, 1993; *Von Damm et al.*, 1995; *Lilley et al.*, 2003], suggesting that Turtle Pits be classified as "immediately post-eruptive."

[26] Examination of the global teleseismic earthquake catalogues shows that the area around 4°48′S was affected by a seismic crisis from 25 to 26 June 2002 (Figure 1b). If the young lava flows seen around Wideawake are related to this earthquake swarm, then the Turtle Pits hydrothermal system has retained its high temperatures and phase separated nature for four years after the magma ascent into the shallow crust. The only other known hydrothermal system with continuous phase separation for several years following an eruption exists at 9°46′N on the East Pacific Rise [*Von Damm et al.*, 1995]; a vent field on the Juan de Fuca ridge, in contrast, showed cessation of

Table 3. Mineralogy of Selected Hydrothermal Precipitates From the Hydrothermal Fields at 4°48′S[a]

Sample	Comment	po	iss	cpy	sl	py/mc	anh	hm	mt	talc	Other
					Turtle Pits						
Active chimneys											
M68/1-12ROV-2	beehive fragments	x	x	x	X	X	–	–	–	–	Fe-ox
M64/1-114ROV-4C1	active beehive	–	–	x	x	**X**	–	–	–	–	–
M64/1-114ROV-4C2	core of active beehive	–	x	**X**	–	x	–	–	–	–	–
M64/1-114ROV-5B2	anhydrite-rich chimney	–	–	x	–	–	**X**	–	–	–	–
M64/1-114ROV-7B	polymetallic chimney	**X**	+	–	+	x	–	–	–	–	Fe-ox
M64/1-123ROV-4C1	anhydrite-rich chimney	–	–	+	–	+	**X**	–	–	–	Fe-ox
M64/1-123ROV-4C2	chimney core	–	X	X	+	x	–	–	–	–	–
M64/1-130ROV-2	polymetallic chimney	**X**	x	–	+	x	–	–	–	–	–
M64/1-141ROV6	polymetallic chimney	**X**	x	–	x	x	+	–	–	–	–
Inactive chimneys											
M64/1-124GTV-2A2	massive pyrite	–	–	x	+	**X**	–	–	–	–	–
M64/1-139GTV-1A1	chalcopyrite conduit	–	–	**X**	+	x	–	–	–	–	–
M64/1-139GTV-1E	chalcopyrite conduit	+	–	**X**	+	x	–	+	–	–	bn, cv
M64/1-139GTV-6A3	polymetallic chimney	–	**X**	x	x	**X**	–	X	+	+	–
M64/1-139GTV-6B2	polymetallic chimney	X	x	x	x	+	–	–	–	–	–
M64/1-139GTV-3C3/2	chimney core	–	–	**X**	+	x	–	–	–	–	–
M64/1-139GTV-3H1	chimney core	–	–	**X**	+	x	–	–	–	–	–
Mound samples											
M68/1-12ROV-1B	massive sulfide	–	X	X	–	X	X	X	x	–	gyp
M64/1-139GTV-2X	massive sulfide	–	–	**X**	–	**X**	–	+	+	–	–
M64/1-139GTV-4H	massive hematite	–	–	+	–	–	–	+	+	**X**	–
M64/1-139GTV-5A2	massive hematite	–	–	+	–	+	–	**X**	+	+	–
M64/1-139GTV-5C3	massive hematite	–	–	–	–	–	–	**X**	**X**	+	–
M64/1-139GTV-5D2	massive hematite	–	–	+	–	x	–	**X**	x	+	–
					Red Lion						
M64/1-146ROV-3	inactive chimney	–	–	+	**X**	X	–	–	–	–	–
M64/1-146ROV-7	flange	–	–	+	+	X	–	–	–	–	–
M68/1-07ROV-1	chimney base	–	+	+	X	X	–	–	–	–	–
M68/1-07ROV-6	chimney wall	–	–	X	+	**X**	–	–	–	–	–
M68/1-07ROV-7	chimney wall	–	–	X	+	**X**	–	–	–	–	–
M68/1-07ROV-8	chimney wall	–	–	X	+	X	–	–	–	–	–
					Comfortless Cove						
M68/1-20ROV-1A	chimney base	–	–	**X**	–	X	–	–	–	–	–
M68/1-20ROV-2	chimney base	–	–	X	–	**X**	–	–	–	–	–
M68/1-20ROV-3A	chimney base	–	–	X	–	**X**	–	–	–	–	clay

[a] Mineralogy based on XRD and microscopy. Abbreviations: anh, anhydrite; bn, bornite; cpy, chalcopyrite; cv, covellite; Fe-ox, fine-grained Fe-oxyhydroxides; hm, hematite; iss, isocubanite; mt, magnetite; po, pyrrhotite; py/mc, pyrite/marcasite; sl, sphalerite.

phase separation within one year after the magmatic event [*Lilley et al.*, 2003].

[27] The strong variations in fluid composition over time concluded for Turtle Pits implies a shallow heat source (in agreement with the Si information) undergoing short-term secular changes rather than a magma lens in several kilometers depth which is relatively stable over hundreds of years [*Lister*, 1983; *Singh et al.*, 2006]. This in turn implies that the present hydrothermal system is linked to a diking and eruption event, such as are observed on faster spreading-ridges [*Delaney et al.*, 1998] rather than to the cooling of a melt lens or a cracking front thought to be more typical for slow-spreading axes [*Wilcock and Delaney*, 1996]. Because heat and the volatile fluxes in hydrothermal fluids depend on the size of the magma body [*Butterfield et al.*, 1997] there must be a relatively large dike beneath the Turtle Pits area. We conclude that volcanic events on the slow-spreading axes have similar effects on hydrothermal systems as eruptions on faster spreading axes although the tectonic and magmatic situations differ significantly.

5.3. Implications for Biogeography

[28] Several distinct biogeographic provinces of hydrothermal vent fauna occur along the mid-

oceanic ridges [*Van Dover et al.*, 2002] with the most significant biogeographic boundary existing between Atlantic and Pacific hydrothermal faunas. Until now, no hydrothermal vents were known from the MAR south of the Equator where the MAR is offset some 1000 km by fracture zones, possibly creating an effective barrier for the southward migration of North Atlantic faunas [*Van Dover*, 1995]. Our findings indicate that although some species common in the next well-known hydrothermal field north of the Equator, the Logatchev field, could not be recorded south of the Equatorial fracture zones (such as the shrimp *Alvinocaris sp.*, galatheid decapods, ophiuroid echinoderms [*Gebruk et al.*, 2000], and zoarcid vent fishes), the 4°48′S hydrothermal area resembles the Logatchev area in its faunal key elements (*Rimicaris exoculata, Bathymodiolus puteoserpentis*). The fauna of the high-temperature vents on the southern MAR also resembles those of other deep-water vent fields on the MAR like Broken Spur, TAG, or Snake Pit [*Copley et al.*, 1997]. A notable exception is the occurrence of vesicomyid clams (*Calyptogena* sp.) in the southern MAR vents which has not been described from the MAR vents north of 20°N. Consequently, we conclude that the large Equatorial offset of the MAR does not represent, as previously postulated, a major faunal barrier and that the biogeographic boundary between Atlantic and East Pacific hydrothermal fauna assemblages must occur further south.

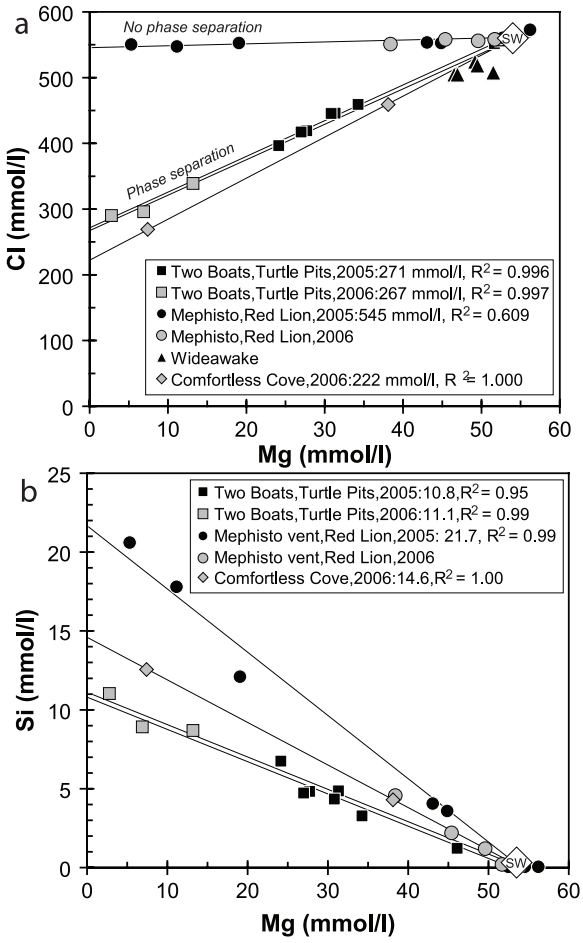

Figure 8. (a) The Cl versus the Mg contents in fluid samples from the different vent fields indicating phase separation and the presence of a vapor phase at Turtle Pits, Comfortless Cove (CC), and Wideawake. No phase separation occurs at Red Lion. The regression lines for the mixing between fluid and seawater (SW) for Turtle Pits and Red Lion fluids as well as the compositions of the end-members (with Mg = 0 mmol/L) and the R^2 values are shown. (b) Si versus Mg contents in vent fluids from 4°48′S. The regression lines for the mixing between fluid and seawater for Turtle Pits, Comfortless Cove, and Red Lion fluids as well as the compositions of the end-members (with Mg = 0 mmol/L) and the R^2 values are shown. Note that there is no change in fluid end-member composition in Turtle Pits from 2005 to 2006.

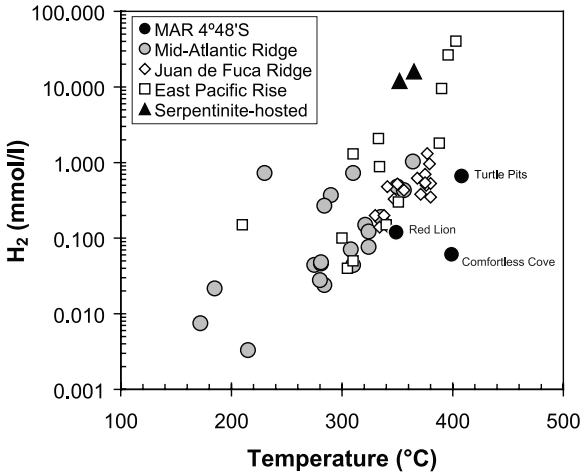

Figure 9. The H_2 concentrations versus the temperature in different end-member fluids from basalt- and serpentinite-hosted hydrothermal vent sites of the Mid-Atlantic Ridge (MAR) [*James et al.*, 1995; *Charlou et al.*, 2000, 2002], the East Pacific Rise, and the Juan de Fuca Ridge [*Charlou et al.*, 1996; *Lilley et al.*, 2003] are shown in comparison to the fluid end-member compositions from the high-temperature vents at 4°48′S. The very high H_2 contents in some fluids from the East Pacific Rise are from the A vent, 9°46.5′N [*Lilley et al.*, 2003].

Acknowledgments

[29] We thank Captain M. Kull and his crew, V. Ratmeyer, C. Seiter and the ROV team from Bremen, the AUV team

from the Woods Hole Oceanographic Institution, and T. Schott for their excellent support on FS Meteor. We gratefully acknowledge the help of G. Seifert and M. Zarrouk with the preparation of the collages of the smoker photographs. A review by D. Butterfield and editorial comments by C. Chauvel led to significant improvements of the manuscript. The work was supported by grants from the priority program SPP1144 of the German Science Foundation (DFG). This is publication 11 of SPP1144 "From Mantle to Ocean: Energy-, Material- and Life-cycles at Spreading Axes."

References

Baker, E. T., and C. R. German (2004), On the global distribution of hydrothermal vent fields, in *Mid-Ocean Ridges: Hydrothermal Interactions Between the Lithosphere and Oceans*, *Geophys. Monogr. Ser.*, vol. 148, edited by C. R. German, J. Lin, and L. M. Parson, pp. 245–266, AGU, Washington, D. C.

Baker, E. T., and H. T. Milburn (1997), MAPR: A new instrument for hydrothermal plume mapping, *RIDGE Events*, *8*, 23–25.

Baross, J. A., M. D. Lilley, and L. I. Gordon (1982), Is the CH_4, H_2 and CO venting from hydrothermal systems produced by thermophilic bacteria?, *Nature*, *298*, 366–368.

Bischoff, J. L., and R. J. Rosenbauer (1988), Liquid-vapor relations in the critical region of the system NaCl-H_2O from 380 to 415°C: A refined determination of the critical point and two-phase boundary of seawater, *Geochim. Cosmochim. Acta*, *52*, 2121–2126.

Butterfield, D. A., I. R. Jonasson, G. J. Massoth, R. A. Feely, K. K. Roe, R. E. Embley, J. F. Holden, R. E. McDuff, M. D. Lilley, and J. R. Delaney (1997), Seafloor eruptions and evolution of hydrothermal fluid chemistry, *Philos. Trans. R. Soc. London, Ser. A*, *355*, 369–386.

Chadwick, W. W., and R. W. Embley (1994), Lava flows from a mid-1980s submarine eruption on the Cleft segment, Juan de Fuca Ridge, *J. Geophys. Res.*, *99*, 4761–4776.

Charlou, J.-L., Y. Fouquet, J.-P. Donval, J. M. Auzende, P. Jean-Baptiste, M. Stievenard, and S. Michel (1996), Mineral and gas chemistry of hydrothermal fluids on an ultrafast spreading ridge: East Pacific Rise, 17° to 19°S (Naudur cruise, 1993) phase separation processes controlled by volcanic and tectonic activity, *J. Geophys. Res.*, *101*, 15,899–15,919.

Charlou, J. L., J. P. Donval, E. Douville, P. Jean-Baptiste, J. Radford-Knoery, Y. Fouquet, A. Dapoigny, and M. Stievenard (2000), Compared geochemical signatures and the evolution of Menez Gwen (37°50′N) and Lucky Strike (37°17′N), hydrothermal fluids, south of the Azores Triple Junction on the Mid-Atlantic Ridge, *Chem. Geol.*, *171*, 49–75.

Charlou, J. L., J. P. Donval, Y. Fouquet, P. Jean-Baptiste, and N. Holm (2002), Geochemistry of high H_2 and CH_4 vent fluids issuing from ultramafic rocks at the Rainbow hydrothermal field (36°14′N, MAR), *Chem. Geol.*, *191*, 345–359.

Christie, D. M., I. S. E. Carmichael, and C. H. Langmuir (1986), Oxidation states of mid-ocean ridge basalt glasses, *Earth Planet. Sci. Lett.*, *79*, 397–411.

Copley, J. T. P., P. A. Tyler, B. J. Murton, and C. L. van Dover (1997), Spatial and interannual variation in the faunal distribution at Broken Spur vent field (29°N, Mid-Atlantic Ridge), *Mar. Biol.*, *129*, 723–733.

De Mets, C., R. G. Gordon, D. F. Argus, and S. Stein (1990), Current plate motions, *Geophys. J. Int.*, *101*, 425–478.

Delaney, J. R., D. S. Kelley, M. D. Lilley, D. A. Butterfield, J. A. Baross, W. S. D. Wilcock, R. W. Embley, and M. Summit (1998), The quantum event of oceanic crustal accretion: Impacts of diking at mid-ocean ridges, *Science*, *281*, 222–230.

Dick, H. J. B., J. Lin, and H. Schouten (2003), An ultraslow-spreading class of ocean ridge, *Nature*, *426*, 405–412.

Ding, K., W. E. Seyfried, M. K. Tivey, and A. M. Bradley (2001), In situ measurement of dissolved H_2 and H_2S in high-temperature hydrothermal vent fluids at the Main Endeavour Field, Juan de Fuca Ridge, *Earth Planet. Sci. Lett.*, *186*, 417–425.

Fornari, D., et al. (2004), Submarine lava flow emplacement at the East Pacific Rise 9°50′N: Implications for uppermost ocean crust stratigraphy and hydrothermal fluid circulation, in *Mid-Ocean Ridges: Hydrothermal Interactions Between the Lithosphere and Oceans*, *Geophys. Monogr. Ser.*, vol. 148, edited by C. R. German, J. Lin, and L. M. Parson, pp. 187–217, AGU, Washington, D. C.

Foustoukos, D. I., and W. E. Seyfried (2007), Quartz solubility in the two-phase and critical region of the NaCl-KCl-H_2O system: Implications for submarine hydrothermal vent systems at 9°50′N East Pacific Rise, *Geochim. Cosmochim. Acta*, *71*, 186–201.

Garbe-Schönberg, D., A. Koschinsky, V. Ratmeyer, H. Jähmlich, and U. Westernströer (2006), KIPS—A new multiport valve-based all-Teflon fluid sampling system for ROVs, paper presented at EGU General Assembly, Eur. Geosci. Union, Vienna.

Gebruk, A. V., P. Chevaldonné, T. Shank, R. A. Lutz, and R. C. Vrijenhoek (2000), Deep-sea hydrothermal vent communities of the Logatchev area (14°45′N, Mid-Atlantic Ridge): Diverse biotopes and high biomass, *J. Mar. Biol. Assoc. U. K.*, *80*, 383–393.

German, C. R., D. P. Connelly, A. J. Evans, and L. M. Parson (2002), Hydrothermal activity on the southern Mid-Atlantic Ridge, *Eos Trans. AGU*, *83*(47), Fall Meeting Suppl., Abstract V61B-1361.

German, C. R., et al. (2005), Hydrothermal activity on the southern Mid-Atlantic Ridge: Tectonically- and volcanically-hosted high temperature venting at 2–7 degrees S, *Eos Trans. AGU*, *86*(52), Fall Meet. Suppl., Abstract OS21C-04.

Haase, K. M., and M64/1 Scientific Party (2005), Hydrothermal venting and volcanism on the southern Mid-Atlantic Ridge, *Eos Trans. AGU*, *86*(52), Fall Meet. Suppl., Abstract OS21C-05.

Haymon, R. (1993), Volcanic eruption of the mid-ocean ridge along the East Pacific Rise crest at 9°45–52′N: Direct submersible observations of seafloor phenomenon associated with an eruption in April 1991, *Earth Planet. Sci. Lett.*, *119*, 85–101.

James, R. H., H. Elderfield, and M. R. Palmer (1995), The chemistry of hydrothermal fluids from the Broken Spur site, 29°N Mid-Atlantic Ridge, *Geochim. Cosmochim. Acta*, *59*, 651–659.

Jannasch, H. W. (1983), Microbial processes at deep sea hydrothermal vents, in *Hydrothermal Processes at Seafloor Spreading Centers*, edited by P. A. Rona et al., pp. 677–701, Plenum, New York.

Kalanetra, K. M., S. L. Huston, and D. C. Nelson (2004), Novel, attached, sulfur-oxidizing bacteria at shallow hydrothermal vents posses vacuoles not involved in respiratory nitrate accumulation, *Appl. Environ. Microbiol.*, *70*, 7487–7496.

Larkin, J. M., and D. L. Shinabarger (1983), Characterization of Thiothrix nivea, *Int. J. Syst. Bacteriol.*, *33*, 841–846.

Lilley, M. D., D. A. Butterfield, J. E. Lupton, and E. J. Olson (2003), Magmatic events can produce rapid changes in hydrothermal vent chemistry, *Nature*, *422*, 878–881.

Lin, J., G. M. Purdy, H. Schouten, J.-C. Sempere, and C. Zervas (1990), Evidence from gravity data for focused magmatic accretion along the Mid-Atlantic Ridge, *Nature*, *344*, 627–632.

Lister, C. R. B. (1983), On the intermittency and crystallization mechanisms of sub-seafloor magma chambers, *Geophys. J. R. Astron. Soc.*, *73*, 351–365.

Lowell, R. P., Y. Yao, and L. N. Germanovich (2003), Anhydrite precipitation and the relationship between focused and diffuse flow in seafloor hydrothermal systems*J. Geophys. Res.*, *108*(B9), 2424, doi:10.1029/2002JB002371.

Moody, J. B. (1976), An experimental study on the serpentinization of iron-bearing olivines, *Can. Mineral.*, *14*, 462–478.

Rehder, G., R. Keir, E. Suess, and M. Rhein (1999), Methane in the northern Atlantic controlled by microbial oxidation and atmospheric history, *Geophys. Res. Lett.*, *26*, 587–590.

Reston, T. J., W. Weinrebe, I. Grevemeyer, E. R. Flueh, N. C. Mitchell, L. Kirstein, and H. Kopp and p. o. M. 47/2 (2002), A rifted inside corner massif on the Mid-Atlantic Ridge at 5°S, *Earth Planet. Sci. Lett.*, *200*, 255–269.

Ruddiman, W. F., and T. R. Janecek (1989), Pliocene-Pleistocene biogenic and terrigenous fluxes at Equatorial Atlantic sites 662, 663, and 664, *Proc. Ocean Drill. Program Sci. Results*, *108*, 211–240.

Sansone, F. J., J. A. Resing, G. W. Tribble, P. N. Sedwick, K. M. Kelly, and K. Hon (1991), Lava-seawater interactions at shallow-water submarine lava flows, *Geophys. Res. Lett.*, *18*, 1731–1734.

Seyfried, W. E. and W. C. Shanks (2004), Alteration and mass transport in mid-ocean ridge hydrothermal systems: Controls on the chemical and isotopic evolution of high-temperature crustal fluids, in *Hydrogeology of the Oceanic Lithosphere*, edited by E. E. Davis and H. Elderfield, pp. 451–495, Cambridge Univ. Press, New York.

Seyfried, W. E., D. I. Foustoukos, and D. E. Allen (2004), Ultramafic-hosted hydrothermal systems at Mid-ocean Ridges: Chemical and physical controls on pH, redox and carbon reduction reactions, in *Mid-ocean Ridges: Hydrothermal Interactions Between the Lithosphere and Oceans*, *Geophys. Monogr. Ser.*, vol. 148, edited by C. R. German, J. Lin, and L. M. Parson, pp. 267–284, AGU, Washington, D. C.

Singh, S. C., W. C. Crawford, H. Carton, T. Seher, V. Combier, M. Cannat, J. P. Canales, D. Dusunur, J. Escartin, and J. M. Miranda (2006), Discovery of a magma chamber and faults beneath a Mid-Atlantic Ridge hydrothermal field, *Nature*, *442*, 1029–1032.

Van Dover, C. L. (1995), Ecology of Mid-Atlantic Ridge hydrothermal vents, in *Hydrothermal Vents and Processes*, edited by L. M. Parson, C. L. Walker, and D. R. Dixon, *Geol. Soc. Spec. Publ.*, *87*, 257–294.

Van Dover, C. L., C. R. German, K. G. Speer, L. M. Parson, and R. C. Vrijenhoek (2002), Evolution and biogeography of deep-sea vent and seep invertebrates, *Science*, *295*, 1253–1257.

Von Damm, K. L. (1995), Controls on the chemistry and temporal variability of seafloor hydrothermal fluids, in *Seafloor Hydrothermal Systems: Physical, Chemical, Biological and Geological Interactions*, *Geophys. Monogr. Ser.*, vol. 91, edited by S. E. Humphris et al., pp. 222–247, AGU, Washington, D. C.

Von Damm, K. L. (2000), Chemistry of hydrothermal vent fluids from 9°–10°N, East Pacific Rise: "Time zero," the immediate posteruptive period, *J. Geophys. Res.*, *105*, 11,203–11,222.

Von Damm, K. L., S. E. Oosting, R. Kozlowski, L. G. Buttermore, D. C. Colodner, H. N. Edmonds, J. M. Edmond, and J. M. Grebmeier (1995), Evolution of East Pacific Rise hydrothermal vent fluids following a volcanic eruption, *Nature*, *375*, 47–50.

Welhan, J. A., and H. Craig (1979), Methane and hydrogen in East Pacific Rise hydrothermal fluids, *Geophys. Res. Lett.*, *11*, 829–831.

White, R. S., D. McKenzie, and R. K. O'Nions (1992), Oceanic crustal thickness from seismic measurements and rare earth element inversions, *J. Geophys. Res.*, *97*, 19,683–19,715.

Wilcock, W. S. D., and J. R. Delaney (1996), Mid-ocean ridge sulfide deposits: Evidence for heat extraction from magma chambers or cracking fronts?, *Earth Planet. Sci. Lett.*, *145*, 49–64.